

## Research Paper

# Mathematical Simulation of Heat Generation at a Cutting-Tool Surface During Stock Removal Processes

Hocine MZAD

*Department of Mechanical Engineering, Badji Mokhtar University of Annaba*

P.O. Box 12, DZ–23000, Algeria

e-mail: h\_mzad@yahoo.fr

ORCID: 0000-0001-9900-6960

The heat generated in various cutting zones significantly influences machining, affects tool wear, and thereby reduces tool life. In this paper, a spline cubic interpolation is used to estimate the transient heat flux imposed on the surface of a carbide cutting tool during stock removal, at constant thermal properties and cutting velocity. Interpolation of instantaneously measured temperature data set by the polynomial of lowest possible degree that passes through the points of the dataset is obtained. A high-precision remote-sensing infrared thermometer is used to measure the temperature at the surface. For friction shear stress determination, a mounted sensing system detects strain gauges signals and computes them in the form of forces on the display screen. From thermal behavior point of view the final result is notably interesting: it highlights the feature of non-proportionality in temperature/heat flux variation.

**Key words:** metal cutting-tool; carbide insert; temperature measurements; polynomial interpolation; TableCurve; heat flux.

## 1. INTRODUCTION

During the machining process, shaping by material removal takes place, which is a complex process that has been the subject of research for a long time. Manufacturers need to optimize their production processes to increase productivity and improve the performance of cutting tools. Temperature is one of the main concerns when choosing process parameters such as cutting speed and feed rate. The significance of temperature prediction in metal cutting has been well recognized in the field of machining for its effects on tool wear and its constraints on productivity. Determining cutting temperature in machining is a major area of research, which was studied in detail at the beginning of the century by TAYLOR [1].

In [2], a new approach for predicting cutting temperature distribution in transient and steady-state heat conduction of TiN-coated tools is compared and

discussed to illustrate the existence of the non-Fourier heat conduction effect in the unsteady-state. With the increase of cutting time, the heat conduction changed from transient-state to steady-state as the cutting temperature stabilized gradually.

In [3], three analytical models have been compared to obtain machining temperatures in orthogonal cutting. The study aimed to promote the use of analytical models in real applications, which provides high prediction accuracy and high computational efficiency.

AUGSPURGER *et al.* [4] published the results of the heat flow distribution between the chip and workpiece in orthogonal cutting processes. A thermodynamic methodology calculated the heat partitions. The thermal diffusivity was included as an evaluation criterion of heat partitioning during cutting different metals at varying undeformed chip thicknesses and cutting velocities.

A finite element modeling (FEM) was employed to predict tool temperature distribution during high-pressure coolant-assisted turning of Inconel 718 [5]. Compared to dry and conventional wet machining, the high pressure jet was able to partially penetrate into the cutting interface, providing both an efficient cooling and lubrication. Analysis of transient and steady-state simulations indicated a significant temperature drop when using high coolant pressure [6].

An experimental temperature measurement technique in dry milling operation with a K-type thermocouple was presented to validate an analytical model proposed to solve the 3D transient heat conduction problem [7]. The model showed that the effect of convection is negligible under dry cutting conditions.

The problem of determining the heat flux  $q$  and heat transfer coefficient  $h$ , based on temperature measurement at three locations in the flat plate, was presented in [8], with the assumption that the material of which the sensor is made is temperature-dependent. The temperature distribution in the analyzed zone was determined using the Gauss-Seidel method and the unknown parameters were determined using the Levenberg-Marquardt method.

A finite difference approach and hybrid analytical-FEM technique allowed predicting the average interface temperatures and their maximum values occurring in dry orthogonal machining of carbon steels with uncoated and coated carbide tools [9]. The comparisons between predicted temperatures and the tool-work thermocouple-based measurements have confirmed the reliability of the proposed models. One of the main findings reveals that the substrate under the thin coating was cooler in comparison to uncoated tools.

SAMADI *et al.* [10] estimated the heat flux in the rake face of a cutting tool by solving the inverse heat conduction problem. Three different thermal conductivity cases were considered, including a temperature dependent-one. The authors have also investigated the effects of sensors locations and nonlinearity of solutions.

LIST *et al.* [11] produced an FEM to explore the dependence of the interface cutting temperature with the crater wear mechanism in the domain of the high-speed machining above 20 m/s. Cutting tests were carried out on a specific ballistic bench equipped with an intensified CCD camera to measure the temperature field of the chip.

High cutting tool temperatures associated with machining titanium alloys have drawn the interest of many researchers. The low thermal conductivity of these alloys is mainly responsible for the heat generated in the primary shear zone. Through an orthogonal cutting of titanium alloy Ti6Al4V, an infrared camera observes the tool-chip interface and measures the temperature distribution [12]. These measurements are relevant because they can be used to validate cutting models. In fact, an improved analytical model of the cutting temperature was proposed based on the Komanduri-Hou model and the Huang-Liang model [13]. The temperatures calculated by the presented model were consistent with the actual cutting temperature field.

In [14, 15], methods were implemented to determine the transient heat transfer at the workpiece-tool interface to optimize metal cutting process. An infrared thermometer and camera were simultaneously used to measure surface temperature and obtained data was modeled using the response surface methodology (RSM) and fuzzy logic (FL). Moreover, a third-order spline approximation was derived for the results treatment.

PATNE *et al.* [16] proposed two thermal models for predicting the temperature distributions in the tool and the workpiece during drilling. To reach the best agreement between simulations and actual results, the authors developed an experimental procedure for the temperature measurements with IR camera assistance.

MIRKOOHI *et al.* [17] used an inverse computational methodology to determine the temperature in the shear zone depending on specific process parameters. A moving point heat source approach allows to obtain adaptively the desirable temperature by optimizing process parameters.

In [18, 19], in order to predict temperature distribution accurately, improved thermal models were presented to simulate an orthogonal cutting process. Challenges were presented through original numerical methods such as smoothed particle hydrodynamics (SPH) and the Johnson-Cook constitutive model (J-C model) regarding convergence properties and boundary treatments [18, 19].

Numerical simulations were performed based on heat transfer models to evaluate the temperature distribution of chip, tool-chip contact, and tool-workpiece contact during high-speed machining processes [20, 21]. Analyzes were conducted on the cutting heat generation and the temperature increment allowing the determination of cutting temperatures. Moreover, the maximum temperature in various cutting zones was successfully simulated.

Cutting strategy depends on the thermophysical properties of the workpiece material. From this point of view, a numerical simulation using finite difference and finite element methods was conducted in [22] to determine and analyze the temperature distribution for an face milled aluminum alloy. It was found that the material surface temperature is mainly affected by heat sources.

GOSAI and BHAVSAR [23] developed an empirical mathematical model of temperature measurement for EN36 as work-piece material, and coated carbide insert as tool material. The authors showed that the change in depth of cut has a very high effect on cutting temperature while cutting speed and feed rate have a moderate effect, which could be very helpful in optimizing the cutting conditions.

In most previous researches, the temperature distribution in machining was investigated with either laborious experiments or complicated numerical simulations. In the present study, to overcome those issues, low experimental complexity of model inputs coupled with a versatile mathematical approach based on preliminary temperature measurements is proposed to determine the heat flux at the cutting tool surface using high precision nonlinear interpolation. Besides, the turning process is performed at a various depths of cut with constant feed and cutting speed. An IR thermometer is positioned at a short distance from the lathe tool equipped with a dynamometer. The present investigation pays attention to the thermal behavior of specified locations on the cutting tool body.

## 2. BRIEF OVERVIEW OF HEAT DISSIPATION IN MACHINING

In machining, mechanical work is converted to heat through the plastic deformation involved in chip formation and through friction between the tool and workpiece. Regions of heat generation in turning are the shear zone, the chip-tool interface and the tool-work piece interface zone. The temperature distribution  $T(x, y, t)$  obeys a transient nonlinear thermal problem in the tool-chip-workpiece system, solved using the heat equation:

$$(2.1) \quad \left( \frac{\partial^2 T}{\partial x^2} + \frac{\partial^2 T}{\partial y^2} \right) + \dot{Q}_{sh} + \dot{Q}_f = \frac{1}{\alpha} \left( \frac{\partial T}{\partial t} + u \frac{\partial T}{\partial x} + v \frac{\partial T}{\partial y} \right).$$

$\dot{Q}_{sh}$  and  $\dot{Q}_f$  are heat sources due to shear and friction, and  $u$  and  $v$  correspond to the velocities in  $x$  and  $y$  directions.

MOLINARI and MOUFKI [24] suggested a thermomechanical model of orthogonal cutting applied to turning operations considering a number of assumptions. He assumed a Hertzian contact of a cylinder applied on a semi-infinite plane with the normal component of the cutting force. Within the chip, the solved heat equation in the steady state case is:

$$(2.2) \quad \frac{k}{\rho c} \frac{\partial^2}{\partial y^2} T(x, y) - u \frac{\partial}{\partial x} T(x, y) = 0.$$

Initial and boundary conditions are:

$$\begin{aligned} T(0, y) &= T_1, & y > 0, \\ T(x, y) &= T_1, & x > 0, \\ -k \frac{\partial T(x, 0)}{\partial y} &= Q, & x > 0. \end{aligned}$$

In Eq. (2.2),  $x$  is parallel to the tool-chip interface and  $y$  is perpendicular.

The mean temperature rise in the shear zone in which the chip is formed is found by OXLEY [25] and expressed as:

$$(2.3) \quad \bar{T}_{sh} = \frac{1 - q_c}{\rho c e_c w} \frac{F_{sh} \cos \alpha}{\cos(\phi - \alpha)},$$

where  $q_c$  is the proportion of heat conducted into the work,  $e_c$  is the undeformed chip thickness,  $w$  is the width of cut measured along the tool cutting edge,  $F_{sh}$  is the shear force,  $\phi$  is the shear angle, and  $\alpha$  is the tool rake angle.

MOUFKI *et al.* [26] developed thermomechanical models in orthogonal and oblique cutting. The authors introduced a friction law that describes the evolution of the apparent friction coefficient as a function of the average temperature at the tool-chip interface:

$$(2.4) \quad \bar{\mu} = \mu_0 \left( 1 - \left( \frac{\bar{T}_{int}}{T_m} \right)^q \right).$$

In the above expression,  $T_m$  represents the material melting temperature,  $\mu_0$  is a friction coefficient of reference, and  $q$  is a parameter controlling the decrease of  $\bar{\mu}$ .

Assuming a perfect sliding contact, the heat generated by friction at the tool-chip interface is estimated:

$$(2.5) \quad Q(x) = \bar{\mu} V_c P(x),$$

$V_c$  is the chip velocity and  $P(x)$  is the interface contact stress expressed as:

$$(2.6) \quad P(x) = P_0 \left( 1 - \frac{x}{l_c} \right)^\xi,$$

$P_0$  is the stress at the tool tip ( $x = 0$ ),  $l_c$  is the length of tool-chip contact, and  $\xi$  is a stress profile coefficient.

The thermal problem within the chip is resolved analytically. The temperature at the tool-chip interface is given by the expression:

$$(2.7) \quad T_{int} = \frac{\bar{\mu} P_0 \sqrt{V_c}}{\sqrt{\pi k \rho c}} \left( \frac{1}{(l_c)^\xi} \sum_{i=0}^{\xi} \frac{2}{2i+1} C_i^\xi (l_c - x)^{\xi-1} x^{\frac{2i+1}{2}} \right) + \theta_h$$

with

$$C_i^\xi = \frac{\xi!}{(\xi - i)! i!},$$

$\theta_h$  is the temperature at the outlet of the primary shear zone. Finally, the temperature  $\bar{T}_{int}$  in Eq. (2.4) is formulated:

$$(2.8) \quad \bar{T}_{int} = \frac{\bar{\mu} P_0 \sqrt{V_c} l_c}{\sqrt{\pi k \rho c}} \sum_{i=0}^{\xi} \frac{2}{2i+1} C_i^\xi \left( \sum_{j=0}^{\xi} (-1)^j C_{\xi-1}^j \frac{2}{2(i+j)+3} \right) + \theta_h.$$

The heat flux at the surface (SHF) is obtained by using the one-dimensional, semi-infinite medium solution for a step change in surface temperature [27]. Duhamel's superposition integral is applied to give:

$$(2.9) \quad \dot{q}(t) = \sqrt{\frac{k \rho c}{\pi}} \int_0^t \frac{dT(\Theta)}{d\Theta} \frac{1}{\sqrt{t-\Theta}} d\Theta,$$

$$(2.10) \quad T(t) = A_0 + A_1 t + A_2 t^2 + \dots + A_m t^m,$$

$T(t)$  is the time-dependent temperature function,  $m$  is polynomial order, and  $\Theta$  is a dummy time variable.

### 3. EXPERIMENTAL METHODOLOGY AND THERMAL PREDICTION

#### 3.1. Experimental methodology

A stock removal during the turning process was accomplished for 20 seconds duration at an ambient temperature around 20°C. The machining tests are carried out on a parallel conventional lathe machine of 7 kW power, and the maximum spindle speed being used is 1250 rpm (Fig. 1a). Experiments measure the tool surface temperature using a high-speed pyrometer under friction coefficient monitoring, thanks to a lathe tool dynamometer. The temperature was captured in an area of about 0.5 cm<sup>2</sup>. The measurements of temperature were repeated seven times according to the friction coefficient, and the resulting average values are reported in Fig. 4. Therefore, 77 measurements were executed in one location, which means a total of 385 temperature measures for the whole experiment.

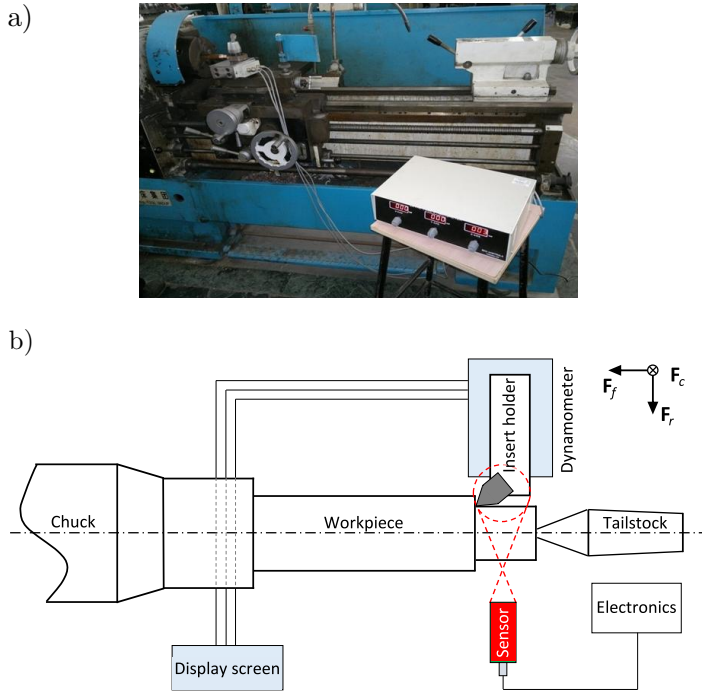


FIG. 1. a) Photo of the lathe machine, b) scheme of the experimental setup of the turning process.

The workpiece material was S235 steel and the insert holder was made of 42CrMo4 steel (Table 1). An uncoated (Cr3C2) carbide tool insert without chip breaker and chamfered cutting edge ( $0.2 \times 20^\circ$ ) was used. Insert holder with negative tool orthogonal rake angle ( $-6^\circ$ ) and tool cutting edge inclination ( $-6^\circ$ ) was used. Furthermore, constant machining parameters of feed rate ( $f = 0.25$  mm/rev) and cutting speed ( $V_c = 250$  m/min) with a variation of depth of cut  $a_p$  (0.8 mm to 2 mm) are implemented. Figure 1b shows the scheme of the experimental setup for the turning operations including temperature and force sensors.

**Table 1.** Materials thermophysical properties at  $20^\circ\text{C}$ .

Parameter	Insert (Cr3C2)	Insert holder (42CrMo4)	Workpiece (S235 steel)
Density, $\rho$ [kg/m <sup>3</sup> ]	6680	7800	7850
Melting temperature, $T_m$ [°C]	1890	1420	1480
Thermal conductivity, $k$ [W/(m·K)]	93.7	46	49–54
Specific heat capacity, $c$ [J/(kg·K)]	450	470	461

Pyrometer is Optris CT 4M (Fig. 3), delivering an output current in the range of 4–20 mA. The temperature interval is  $[273, 773]$  in K for a spectral range of 2.2–6  $\mu\text{m}$ . The sensing head is a cylinder approximately 3 cm long, 1.5 cm in diameter and a mass of 40 g. Electronics (box and wire) weight is 420 g. The temperature resolution is 120 mK, the accuracy of 0.3% at an ambient temperature of  $23 \pm 5^\circ\text{C}$  and the response time (at 90%) is 300  $\mu\text{s}$ . The measurement distance between the pyrometer and the tooltip is 10 cm. The temperature capture is focused on five specified locations on the tool body surface (Fig. 2), from zone A to zone E.

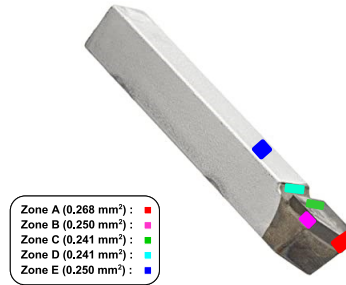


FIG. 2. Tested cutting tool.



FIG. 3. Pyrometer Optris CT 4M.

### 3.2. Data processing and thermal prediction

Every single point located on the tool surface is studied separately, and the curve data describing the instantaneous temperature measurements (Fig. 4) are

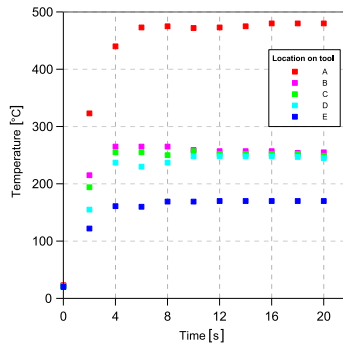


FIG. 4. Temperature data measurements.

exported to TableCurve 2D V5.01 software for a non-linear curve fitting. Graphs (Fig. 5) show results of a high-precision fifth-order polynomial interpolation of the temperature variation in time.

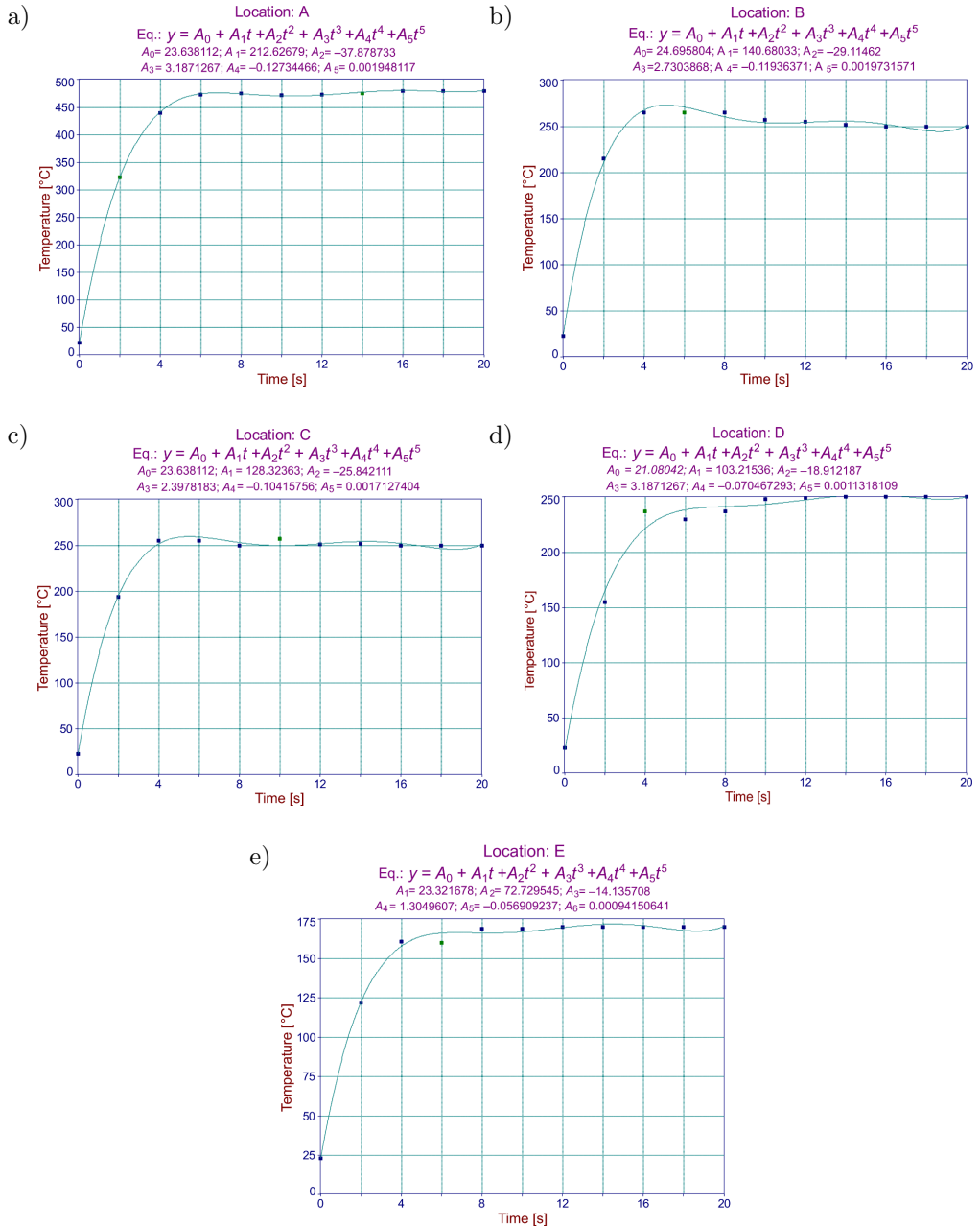


FIG. 5. Polynomial interpolation of temperature.

The investigative thermal procedure plots the actual tool body temperatures at different locations represented by colors, as shown in Fig. 2. Temperature history is then related to the one of heat transfer rate. Replacing the polynomial function (Eq. 2.10) into Eq. (2.9) and its integrating yields the formulation of the surface heat flux  $\dot{q}(t)$  in a semi-infinite body [27]:

$$(3.1) \quad \dot{q}(t) = 2\sqrt{\frac{\lambda \rho c}{\pi}} \left\{ A_1 \sqrt{t} + \sum_{i=2}^m i A_i t^{\frac{2i-1}{2}} \left[ 1 + (i-1)! \sum_{k=1}^{i-1} \frac{(-1)^k}{(2k+1)k!(i-1-k)!} \right] \right\}.$$

Therefore, according to the above polynomial interpolation ( $m = 5$ ), the resultant algebraic equation is solved to find the time-varying heat flux (Fig. 6):

$$(3.2) \quad \dot{q}(t) = 2\sqrt{\frac{\lambda \rho c}{\pi}} \left( A_1 \sqrt{t} + \frac{4}{3} A_2 \sqrt{t}^3 + \frac{8}{5} A_3 \sqrt{t}^5 + \frac{64}{35} A_4 \sqrt{t}^7 + \frac{128}{63} A_5 \sqrt{t}^9 \right).$$

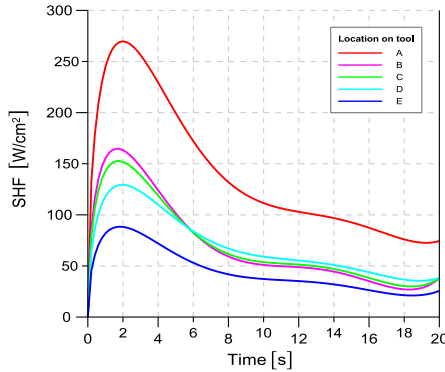


FIG. 6. Surface heat flux of the tested cutting tool.

#### 4. SYNOPSIS AND RESULTS INTERPRETATION

A considerable number of temperature measures were used to predict the cutting tool's local heat flux while metal is removed. The undertaken experimental protocol combines parameters that influence heat dissipation in the cutting zone, namely material thermophysical properties, cutting speed, feed and depth of cut. In the present study, the quantification of the heat flow distribution in the metal cutting process concerns carbide tool insert (Zones A, B, and C) and insert holder (Zones D and E).

A lathe dynamometer rigidly mounted on the tool post where the cutting tool is fixed, is used to measure the cutting forces coming to the tooltip. The sensor measures the forces accurately without loss of the force. Forces in  $x$ ,  $y$ ,  $z$

directions are shown individually and simultaneously in three digital indicators supplied (Table 2).

**Table 2.** Measured forces and resultant friction coefficient,  $a_p = (0.8-2)$  mm.

$F_r$ [N]	71.6	89.5	107.6	125.4	143.4	161	179
$F_f$ [N]	98.4	125.9	154.9	184.8	216.1	247.9	281.6
$F_c$ [N]	238.8	298.3	358.7	418.1	478.1	536.6	596.6
$\mu$	0.412	0.422	0.432	0.442	0.452	0.462	0.472

In order to evaluate the friction factor ( $\mu$ ), the process of stock removal was assumed to obey Coulomb's law of friction. In this case, the ratio of the feed force ( $F_f$ ) to the cutting force ( $F_c$ ) leads to the friction factor values given in Table 2.

The temperature distribution in the whole tool, including insert closer to the cutting edge, is shown in Figs 4 and 5. Because of better distinction, the experimental results obtained for the selected zones are reported in one single figure (Fig. 4). These results are then illustrated individually by the fifth-order polynomial interpolation of the temperature (Fig. 5). The maximum interface temperature, in dry cutting, exists in the vicinity of the cutting edge, i.e., in the first part of the tool-chip contact. However, significant temperature decreases were recorded from the tooltip because of less duration of heat impact. Obviously, as shown in the results obtained, the temperature decreases when moving away from the machining zone. At the too tip (Zone A), temperature evolves in two stages. From 0 to 6 s, the first step corresponds to an abrupt increase in temperature up to a maximum value,  $T_{\max} = 477^\circ\text{C}$ . After that, the temperature stabilizes around  $T_{\max}$  with a tiny fluctuation of more or less  $5^\circ\text{C}$ . For the other measurement points, the first step happens from 0 to 4 s but with similar temperature evolution.

The two main heat sources in cutting processes are the plastic work and the dissipation of friction energy at the tool-chip interface, which are practically fully converted into heat. The heat flux of friction and heat of plastic deformation, which strongly depend on the contact temperature, are incorporated into the predicted SHF. The surface temperature propagated to the tool is integrated, and the heat transfer rate of the tool surface (SHF) is deduced. Figure 6 shows the heat flux behavior in the selected positions on the cutting tool. Oddly, the result does not completely match with the aforementioned temperature evolution. This feature proves that the heat generated within the tool does not necessary vary with the temperature. The maximum heat flux in the tooltip,  $\dot{q}_{\max}(t) = 270 \text{ W/cm}^2$ , occurs for  $T = 323^\circ\text{C}$  when  $t = 2$  s. After that, the flux decreases to reach a value of about  $70 \text{ W/cm}^2$  in 20 seconds. Further move away

from the machining zone implies lower heat fluxes. The duration of machining and heat evacuation speed shortens the influence of the thermal fluxes on the cutting insert. As a result, the total amount of heat penetrating the cutting tool is significantly reduced.

All cutting actions occur at the edge of the tool; the dislocation deformations of materials will transfer potential energy into the kinetic energy and result in a temperature rise. The thermal conductivity and specific heat of the carbide cutting insert material are a function of temperature. In [28], it was shown that thermal diffusivity decreases by 25% within the temperature range 20–600°C. However, due to the short machining time of 20 s, it should be noted that these calculations were carried out for the thermal diffusivities of 0.312 cm<sup>2</sup>/s for the carbide insert and 0.125 cm<sup>2</sup>/s for the insert holder.

## 5. CONCLUSIONS

This paper studied the effect of increasing cut depth at constant cutting speed and feed during the dry material removal process on the involved thermal energy of friction and plastic deformation. The SHF behavior was highlighted in the partitions selected on the cutting tool. Based on the results, the following conclusions can be made:

- A simple mathematical technique of heat measurement was presented for 42CrMo4 as insert holder material and Cr2C3 uncoated carbide insert as cutting tool material.
- The high heat flux was reached at  $t = 2$  s, it was of the order of 270 W/cm<sup>2</sup>, and a decrease of 50% was recorded after 10 s. The fast heat dissipation was due to heat transferred by convection with the surroundings. The remaining time, until  $t = 20$  s, the high-speed machining process exhibits lower heat fluxes because of less duration of heat impact.
- The accuracy of the thermal results depends on reliable force measurements, i.e., the ratio ( $F_f/F_c$ ). As there is no drift in the force measurement, inferred values of friction coefficient  $\mu$  falling between 0.412 ( $a_p = 0.8$  mm) and 0.472 ( $a_p = 2$  mm) do not affect the final result.

## REFERENCES

1. TAYLOR F.W., *On the Art of Cutting Metals*, The American Society of Mechanical Engineers, NY, 1907.
2. ZHANG J., MENG X., DU J., XIAO G., CHEN Z., YI M., XU C., Modelling and prediction of cutting temperature in the machining of H13 hard steel of transient heat conduction, *Materials*, **14**(12): 3176, 2021, doi: 10.3390/ma14123176.

3. NING J., LIANG S.Y., A comparative study of analytical thermal models to predict the orthogonal cutting temperature of AISI 1045 steel, *The International Journal of Advanced Manufacturing Technology*, **102**: 3109–3119, 2019, doi: 10.1007/s00170-019-03415-9.
4. AUGSPURGER T., BERGS T., DOBBELER B., Measurement and modeling of heat partitions and temperature fields in the workpiece for cutting Inconel 718, AISI 1045, Ti6Al4V, and AlMgSi0.5, *Journal of Manufacturing Science and Engineering*, **141**(6): 061007, 2019, doi: 10.1115/1.4043311.
5. D'ADDONA D.M., RAYKAR S.J., Thermal modeling of tool temperature distribution during high pressure coolant assisted turning of Inconel 718, *Materials*, **12**(3): 408, 2019, doi: 10.3390/ma12030408.
6. MZAD H., KHELIF R., Effect of spraying pressure on spray cooling enhancement of beryllium-copper alloy plate, *Procedia Engineering*, **157**: 106–113, 2016, doi: 10.1016/j.proeng.2016.08.344.
7. KARAGUZEL U., BAKKAL M., BUDAK E., Modeling and measurement of cutting temperatures in milling, *Procedia CIRP*, **46**: 173–176, 2016, doi: 10.1016/j.procir.2016.03.182.
8. TALER D., GRADZIEL S., TALER J., Measurement of heat flux density and heat transfer coefficient, *Archives of Thermodynamics*, **31**(3): 3–18, 2010, doi: 10.2478/v10173-010-0011-z.
9. GRZESIK W., Determination of temperature distribution in the cutting zone using hybrid analytical-FEM technique, *International Journal of Machine Tools and Manufacture*, **46**(6): 651–658, 2006, doi: 10.1016/j.ijmachtools.2005.07.009.
10. SAMADI F., KOWSARY F., SARCHAMI A., Estimation of heat flux imposed on the rake face of a cutting tool: A nonlinear complex geometry inverse heat conduction case study, *International Communications in Heat and Mass Transfer*, **39**(2): 298–303, 2012, doi: 10.1016/j.icheatmasstransfer.2011.10.007.
11. LIST G., SUTTER G., BOUTHICHE A., Cutting temperature prediction in high speed machining by numerical modelling of chip formation and its dependence with crater wear, *International Journal of Machine Tools and Manufacture*, **54–55**: 1–9, 2012, doi: 10.1016/j.ijmachtools.2011.11.009.
12. HEIGEL J.C., WHITENTON E., LANE B., DONMEZ M.A., MADHAVAN V., MOSCOSO-KINGSLEY W., Infrared measurement of the temperature at the tool-chip interface while machining Ti-6Al-4V, *Journal of Materials Processing Technology*, **243**: 123–130, 2017, doi: 10.1016/j.jmatprotec.2016.11.026.
13. SHAN C., ZHANG X., SHEN B., ZHANG D., An improved analytical model of cutting temperature in orthogonal cutting of Ti6Al4V, *Chinese Journal of Aeronautics*, **32**(3): 759–769, 2019, doi: org/10.1016/j.cja.2018.12.001.
14. MZAD H., A simple mathematical procedure to estimate heat flux in machining using measured surface temperature with infrared laser, *Case Studies in Thermal Engineering*, **6**: 128–135, 2015, doi: 10.1016/j.csite.2015.09.001.
15. TANIĆ D., MARINKOVIĆ V., MANIĆ M., DEVEDŽIĆ G., RANDELOVIĆ S., Application of response surface methodology and fuzzy logic based system for determining metal cutting temperature, *Bulletin of the Polish Academy of Sciences: Technical Sciences*, **64**(2): 435–445, 2016, doi: 10.1515/bpasts-2016-0049.
16. PATNE H.S., KUMAR A., KARAGADDE S., JOSHI S.S., Modeling of temperature distribution in drilling of titanium, *International Journal of Mechanical Sciences*, **133**: 598–610, 2017, doi: 10.1016/j.ijmecsci.2017.09.024.

17. MIRKOOHI E., BOCCHINI P., LIANG S.Y., Analytical temperature predictive modeling and non-linear optimization in machining, *The International Journal of Advanced Manufacturing Technology*, **102**: 1557–1566, 2019, doi: 10.1007/s00170-019-03296-y.
18. NING J., LIANG S.Y., Prediction of temperature distribution in orthogonal machining based on the mechanics of the cutting process using a constitutive model, *Journal of Manufacturing and Materials Processing*, **2**(2): 37, 2018, doi: 10.3390/jmmp2020037.
19. AFRASIABI M., KLIPPEL H., ROETHLIN M., WEGENER K., Smoothed particle hydrodynamics simulation of orthogonal cutting with enhanced thermal modeling, *Applied Sciences*, **11**(3): 1020, 2021, doi: 10.3390/app11031020.
20. KUMAR A., BHARDWAJ R., JOSHI S.S., A finite-element heat transfer model for orthogonal cutting, *Advances in Materials and Processing Technologies*, **6**(4): 686–702, 2020, doi: 10.1080/2374068X.2020.1741059.
21. SU G., XIAO X., DU J., ZHANG J., ZHANG P., LIU Z., XU C., On cutting temperatures in high and ultrahigh-speed machining, *The International Journal of Advanced Manufacturing Technology*, **107**: 73–83, 2020, doi: 10.1007/s00170-020-05054-x.
22. NOWAKOWSKI L., SKRZYNIARZ M., BLASIAK S., BARTOSZUK M., Influence of the cutting strategy on the temperature and surface flatness of the workpiece in face milling, *Materials*, **13**(20): 4542, 2020, doi: 10.3390/ma13204542.
23. GOSAI M., BHAVSAR S.N., Experimental study on temperature measurement in turning operation of hardened steel (EN36), *Procedia Technology*, **23**: 311–318, 2016, doi: 10.1016/j.protcy.2016.03.032.
24. MOLINARI A., MOUFKI A., A new thermomechanical model of cutting applied to turning operations. Part I. Theory, *International Journal of Machine Tools and Manufacture*, **45**(2): 166–180, 2005, doi: 10.1016/j.ijmachtools.2004.07.004.
25. OXLEY P.L.B., *The Mechanics of Machining: An Analytical Approach to Assessing Machinability*, Ellis Horwood Ltd., Chichester, UK, 1989.
26. MOUFKI A., DEVILLEZ A., DUDZINSKI D., MOLINARI A., Thermomechanical modeling of oblique cutting and experimental validation, *International Journal of Machine Tools and Manufacture*, **44**(9): 971–989, 2004, doi: 10.1016/j.ijmachtools.2004.01.018.
27. TALER J., Theory of transient experimental techniques for surface heat transfer, *International Journal of Heat and Mass Transfer*, **39**(17): 3733–3748, 1996, doi: 10.1016/0017-9310(96)00015-4.
28. BARTOSZUK M., Temperature and heat partition testing in the cutting zone for turning AISI 321 steel, *Strojniški Vestnik – Journal of Mechanical Engineering*, **66**(11): 629–641, 2020, doi: 10.5545/sv-jme.2020.6840.

Received July 21, 2021; accepted version November 25, 2021.

Published on Creative Common licence CC BY-SA 4.0

